SCIENCE CHINA
Physics, Mechanics & Astronomy

• Research Paper •

November 2011 Vol.54 No.11: 1981–1989
doi: 10.1007/s11433-011-4516-5

An electron momentum spectroscopic study of naphthalene in gas phase

SHI LeLei, LIU Kun, NING ChuanGang* & DENG JingKang*

Department of Physics, State Key Laboratory of Low-Dimensional Quantum Physics, Tsinghua University, Beijing 100084, China

Received March 10, 2011; accepted June 29, 2011; published online September 27, 2011

We report the experimental and theoretical investigation of the complete valence shell binding energy spectra and momentum profiles of naphthalene ($C_{10}H_8$), using our high resolution electron momentum spectrometer, at impact energies of 1500 eV and 600 eV. The observed momentum profiles were compared with the Hartree-Fock (HF) and density functional theory (DFT) calculations, and the binding energy spectrum was compared with the Outer valence Green's function (OVGF) calculations. The impact energy dependent discrepancy between observed momentum distributions and calculations under the plane wave impulse approximation was ascribed to the distorted wave effects.

naphthalene, EMS, distorted wave effects

PACS: 34.80.Gs, 31.15.aj

1 Introduction

Electron momentum spectroscopy (EMS) [1–3], also named (e, 2e) spectroscopy, is based on the kinetics complete electron impact ionization process. Besides the detailed information on the binding energies, the momentum profiles, i.e., the orbital electron density distributions of atoms and molecules in the momentum space can be also observed. This unique ability has made EMS a powerful tool for investigating the electronic structures of atoms, molecules and solids.

Naphthalene is a crystalline, aromatic, white, solid hydrocarbon with a formula $C_{10}H_8$ and the structure of two fused benzene rings. It is best known as the primary ingredient of mothballs because it is volatile and readily sublimes at room temperature. This feature made naphthalene an ideal molecular target for the gas phase EMS study. Naphthalene is also one of the fundamental structures in the stereochemistry of organic compounds. In the present work, we investigated the electronic structure of this important prototype molecule using the EMS method. Several studies of molecular structure and photoelectron spectroscopy have been reported [4–9]. Klevens and Platt firstly assigned the ultraviolet spectra of naphthalene in *n*-heptane solution in 1949 [4]. Vanbrunt and Wacks used the Electron-Impact method to study this compound in 1964 [5]. The photoelectron spectrum of naphthalene in gas phase, was first reported by Munakata et al. in 1981 [6], and then by Yamauchi et al. in 1998 [7], which was compared with our EMS research in this paper. In the 1990s, photofragmentation of naphthalene and its isomer was carried out by Jochims et al. [8]. In recent years, Rink and Boesl identified mass-selected resonance-enhanced multiphoton ionization spectra of this molecule [9].

This work reported the momentum distributions of the orbitals of naphthalene measured at the impact energies of 600 eV and 1500 eV plus binding energies. The experimental momentum profiles were compared with both the Hartree-Fock (HF) and density functional theory (DFT) calculations using Aug-cc-pVTZ [10] and 6-311++G** [11] basis sets.

*Corresponding author (email: ningcg@tsinghua.edu.cn; djk-dmp@tsinghua.edu.cn)

2 Theoretical background

The relative (e, 2e) cross-section for electron impact ionization in EMS is measured by detecting the two outgoing electrons in coincidence. In our spectrometer, the symmetric non-coplanar kinematics [1,3,12] is used, which is the most common experimental configuration for the study of electronic structures. In this kinematics, the scattered and ionized electrons are detected in coincidence at almost equal kinetic energies and equal polar angles, i.e. $E_1 \approx E_2$, and $\theta_1 \approx \theta_2 = 45°$, and therefore almost equal momenta $p_1=p_2$. The initial momentum p of the electron before knocked-out is determined through the out-of-plane azimuthal angle φ between the two outgoing electrons by [3]:

$$p = \left[\left(2p_1 \cos\theta_1 - p_0 \right)^2 + 4{p_1}^2 \sin^2\theta_1 \sin^2\left(\frac{\varphi}{2} \right) \right]^{1/2}, \quad (1)$$

where p_0 is the momentum of the incident electron.

Under the conditions of the high impact energy, high-momentum transfer, and negligible kinetic-energy transfer to the residual ion, the plane wave impulse approximation (PWIA) presents a good description for the collision. With the PWIA, the EMS differential cross section for randomly oriented gas-phase molecules is given by [1]

$$\sigma_{\mathrm{EMS}} \propto \frac{1}{4\pi} \int \mathrm{d}\Omega \left| \left\langle \mathrm{e}^{-\mathrm{i}\boldsymbol{p}\cdot\boldsymbol{r}} \Psi_f^{N-1} \middle| \Psi_i^N \right\rangle \right|^2, \quad (2)$$

where $\mathrm{e}^{-\mathrm{i}\boldsymbol{p}\cdot\boldsymbol{r}}$ is the plane wave for electrons, and $\left|\Psi_f^{N-1}\right\rangle$ and $\left|\Psi_i^N\right\rangle$ are the wave functions for the final ion state and the target molecule ground (initial) state, respectively. N is the total electron number. Using the target Hartree-Fock approximation (THFA) or the target Kohn-Sham approximation (TKSA) [13], eq. (2) can be reduced to

$$\sigma_{\mathrm{EMS}} \propto \int \mathrm{d}\Omega \left| \psi_j(\boldsymbol{p}) \right|^2, \quad (3)$$

where $\psi_j(\boldsymbol{p})$ is the momentum space Hartree-Fock or Kohn-Sham orbital for the jth electron. The integral in eq. (3) is known as the spherically average single electron momentum distribution. Thus, the electron density of individual orbital can be featured according to their binding energies.

3 Experimental methods

The details of our high resolution EMS spectrometer constructed at Tsinghua University have been previously reported elsewhere [14,15]. In short, the spectrometer takes the symmetric non-coplanar geometry in which the target is ionized by a high energy electron beam. The electron beam with a low energy spread and small divergence angle is generated by an electron gun with an oxide cathode. For keeping the high vacuum required by the oxide cathode, the electron gun is installed in an additional chamber, which can be evacuated to a base pressure of 10^{-6} Pa by a 600 L/s molecular turbo pump. The energy resolution depends on the emitting current of the cathode due to the space charge effects. The typical energy resolution is 0.68 eV (full width at half maximum, FWHM) at the impact energy 1200 eV. With a double toroidal energy analyzer and two large position sensitive detectors, the collecting efficiency for the coincidental (e, 2e) events is much higher than our previous spectrometer.

The naphthalene sample is a commercial product with a purity of 99.0%. The sample is solid, and can sublime at room temperature. Since the volatility is not sufficient, the sample was put inside the spectrometer with a sample probe near the collision region. A heater with a variable power, typically 0.4 W, was used to control the density of gaseous molecules. No further purification was processed during the measurements, and no impurity of the sample was observed in the binding energy spectra evidently.

4 Results and discussion

The naphthalene ($C_{10}H_8$) molecule has D_{2h} point group symmetry. The orbital ordering for outer valence orbitals was calculated using outer valence Green's function (OVGF) with 6-311++G** basis set [16–20], while for the inner valence orbitals, DFT was taken by using statistic averaged orbital potential (SAOP) with the TZ2P basis set [21]. According to the calculated results, the ground state electronic configuration can be written as:

$$(Core)^{20} \underbrace{\left(4a_g\right)^2 \left(3b_{2u}\right)^2 \left(4b_{1u}\right)^2 \left(5a_g\right)^2 \left(3b_{3g}\right)^2 \left(4b_{2u}\right)^2 \left(5b_{1u}\right)^2 \left(6a_g\right)^2}_{\text{Inner valence}},$$

$$\underbrace{\left(4b_{3g}\right)^2 \left(5b_{2u}\right)^2 \left(7a_g\right)^2 \left(6b_{1u}\right)^2 \left(8a_g\right)^2 \left(5b_{3g}\right)^2 \left(6b_{2u}\right)^2 \left(7b_{1u}\right)^2 \left(1b_{3u}\right)^2 \left(7b_{2u}\right)^2 \left(6b_{3g}\right)^2 \left(9a_g\right)^2 \left(1b_{1g}\right)^2 \left(1b_{2g}\right)^2 \left(2b_{3u}\right)^2 \left(1a_u\right)^2}_{\text{Outer valence}}.$$

In the ground state, the 68 electrons are arranged in 34 double-occupied orbitals in the independent particle description. The valence shell of naphthalene which contains 24 molecular orbitals can be divided into two sets: 8 inner valence and 16 outer valence orbitals.

The binding energy spectrum of naphthalene in the range of 5–30 eV at the electron impact energy of 1500 eV was shown in Figure 1(b). With the reference to the high resolu-

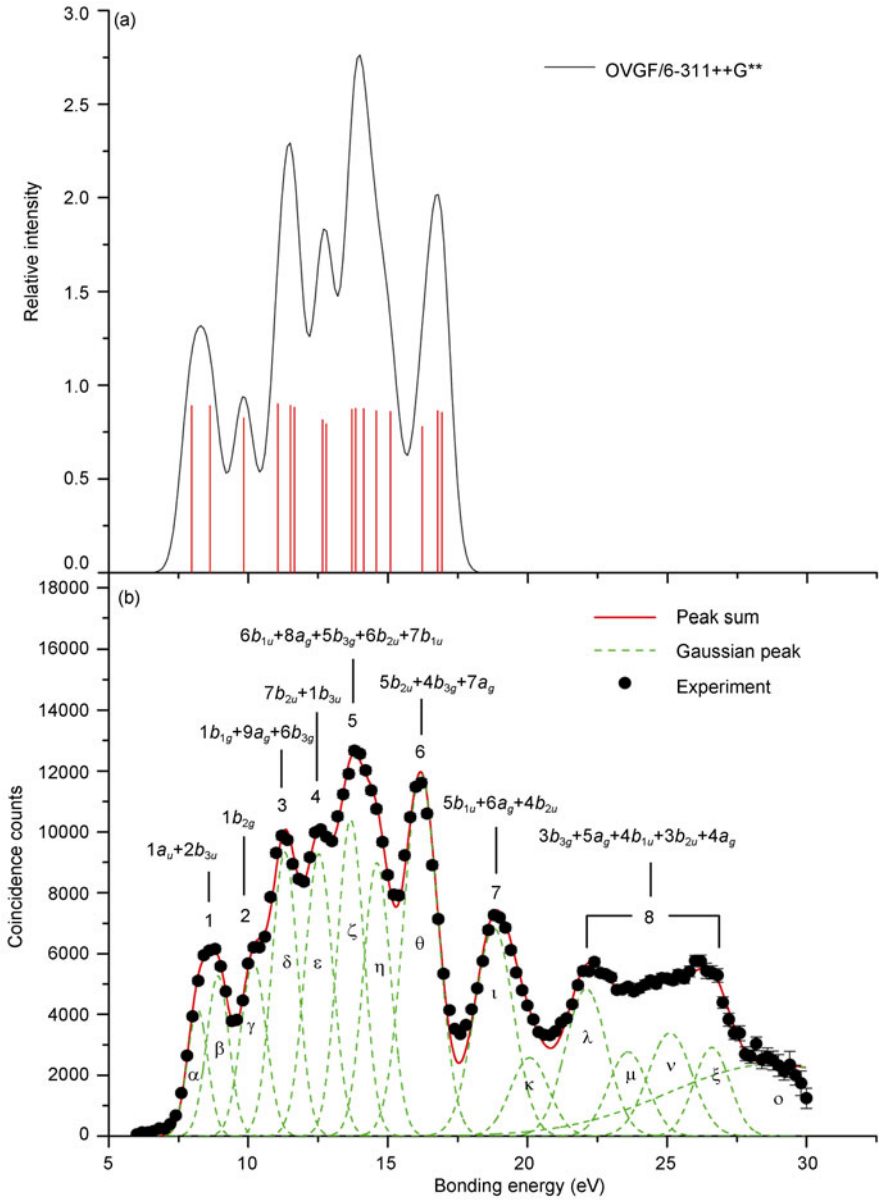

Figure 1 (Color online) (a) The theoretical simulation of binding energy spectra of naphthalene. The vertical bars under the curve are the OVGF/6-311++G** results. A common width (0.88 eV FWHM) was used in the simulation; (b) experimental binding energy spectrum summed over all azimuthal angles at impact energies of 1500 eV plus binding energies. The dashed and solid curves represent individual and summed Gaussian fits, respectively. The error bars represent one standard deviation.

tion PES and the OVGF calculation, there are seven resolved structures which are labeled as 1–7 as well as the orbital assignment in this figure. In order to obtain the experimental momentum distributions, the binding energy spectra at different angles were fitted by Gaussian peaks, as the dashed and solid curves indicated in Figure 1. The clusters of humps in the inner valence region (higher than 20 eV and lower than 30 eV) are the results of the congested satellite lines in this region due to the breakup of orbital pictures [22].

In order to assign the observed binding energy spectra, binding energy spectra were theoretically simulated by the OVGF method with the basis sets of 6-311++G**, as shown in Figure 1(a). The simulated spectra were obtained by convoluting the contributions from each line (given in Table 1) with a Gaussian shape function with a common width 0.88 eV (FWHM), which approximated the vibrational broadening and the energy resolution of the spectrometer. The heights of vertical bars under the curve represent the pole strengths given by OVGF. It can be seen that the simulated spectra of naphthalene agree with the experimental binding energy spectrum in both peak positions and intensities in the outer valence space (<18 eV). For assigning the inner valence orbitals, DFT-SAOP/TZ2P method was

Table 1 Ionization energies of naphthalene (in eV)

Peak	EMS	PES[a] (HeI)	PES[b] (HeI)	Fit[c]	OVGF/ 6-311++G**	SAOP/TZ2P	Orbital
1	8.6	8.3	8.00	8.18 (α)	7.96 (0.890)	9.470	$1a_u$
		9.0	8.80	8.91 (β)	8.62(0.887)	10.140	$2b_{3u}$
2	10.2	10.1	9.99	10.2 (γ)	9.84(0.872)	11.038	$1b_{2g}$
			10.85		11.06(0.824)	12.059	$1b_{1g}$
3	11.2	11.0	11.4	11.2 (δ)	11.51 (0.895)	11.929	$9a_g$
			11.7		11.65 (0.892)	12.055	$6b_{3g}$
4	12.5	12.4	12.22	12.5 (ε)	12.66 (0.882)	12.871	$7b_{2u}$
			12.41		12.79 (0.793)[d]	13.557	$1b_{3u}$
			13.32	13.67 (ξ)	13.71 (0.873)	13.708	$7b_{1u}$
			13.6		13.84 (0.876)	14.009	$6b_{2u}$
5	14.0		14.0		14.13 (0.875)	14.101	$5b_{3g}$
			14.4	14.61 (η)	14.58 (0.863)	14.675	$8a_g$
			14.8		15.09 (0.858)	14.924	$6b_{1u}$
			15.85		16.22 (0.779)[d]	16.013	$7a_g$
6	16.2		16.3	16.2 (θ)	16.78(0.863)	16.577	$5b_{2u}$[e]
			16.8		16.93(0.854)	16.509	$4b_{3g}$[e]
			18.7	18.80 (ι, 0.75)		18.683	$6a_g$
7	19.0		18.7			19.043	$5b_{1u}$
			18.7	20.08 (κ, 0.75)		19.400	$4b_{2u}$
				22.10 (λ, 0.44)		21.812	$3b_{3g}$
						22.342	$5a_g$
8	26.0			23.60 (μ, 0.4)		23.140	$4b_{1u}$
				25.10 (ν, 0.44)		24.362	$3b_{2u}$
				26.60 (ξ, 0.14)		25.694	$4a_g$

a) From ref. [6];

b) From ref. [7];

c) The centers of fitting Gaussian peaks, which have been labeled in Figure 1(b) with Greek letters α, β, γ… Pole strengths of outer-valence orbitals in our rescaling of experimental intensities are assumed equal to 1. The pole strengths of the inner valence orbitals $6a_g$ +$5b_{1u}$, $4b_{2u}$, $3b_{3g}$+$5a_g$, $4b_{1u}$, $3b_{2u}$ and $4a_g$ were 0.75, 0.75, 0.44, 0.4, 0.44 and 0.14, respectively;

d) The calculated pole strength is not accurate by OVGF when it is less than 0.8;

e) The ionization energy of molecular orbital $4b_{3g}$ is higher than $5b_{2u}$ in our OVGF calculation which is different from ref. [7].

used to calculate the ionization potentials (I.P.). SAOP can predict I.P. with reasonable accuracy since it corrects the asymptotic error of the general exchange correlation potential X_c.

The experimental momentum profiles were extracted by deconvolving the same peak from the obtained binding energy spectra at different azimuthal angles [3]. The centers and widths of those Gaussian functions were first determined through the high-resolution PES [14], and then adjusted for compensating the asymmetries in the shape of Franck–Condon envelopes. Theoretical momentum profiles have been convolved with the experiment momentum resolution at E_0 = 1500 eV using the Monte Carlo method [23]. Since the experimental intensity is at a relative scale, a normalization procedure is needed for comparing the experimental momentum distributions (MD) with the theoretical counterparts. Here, we normalized the experimental orbital MDs through the summation of the experimental MDs in the outer region, i.e. peaks 1–6 in the binding energy spectrum (see Figure 1) for the best fitting with the corresponding summation of theoretical molecular orbitals of naphthalene. The obtained normalization factor was also used to calculate the pole strengths of inner valence orbitals.

Figure 2 shows the experimental momentum distribution of peak 1, peak 2 and peak 3 at impact energies of 600 and 1500 eV in comparison with four theoretical momentum profiles calculated using HF and DFT-B3LYP methods with the Aug-cc-pVTZ and 6-311++G** basis sets. It can be seen that the four different calculations are nearly the same and reasonably describe the experimental momentum distributions.

The first peak is located at 8.6 eV and contains two molecular orbitals, the highest occupied molecular orbital (HOMO, $1a_u$) and the next-highest occupied molecular orbital (N-HOMO, $2b_{3u}$) (see Figure 1). Both orbitals are of typical *p*-type, which has near zero intensity at momentum origin p = 0 a.u. and maximum intensity at $p \approx 0.75$ a.u. The theoretical calculations are in good agreement with experimental data except the region around the momentum origin ($p < 0.5$ a.u.).

Peak 2, located at 10.2 eV, is related to the molecular orbital $1b_{2g}$, as shown in Figure 1. The momentum distributions of $1b_{2g}$ also display a typical *p*-type. Peak 3 is located

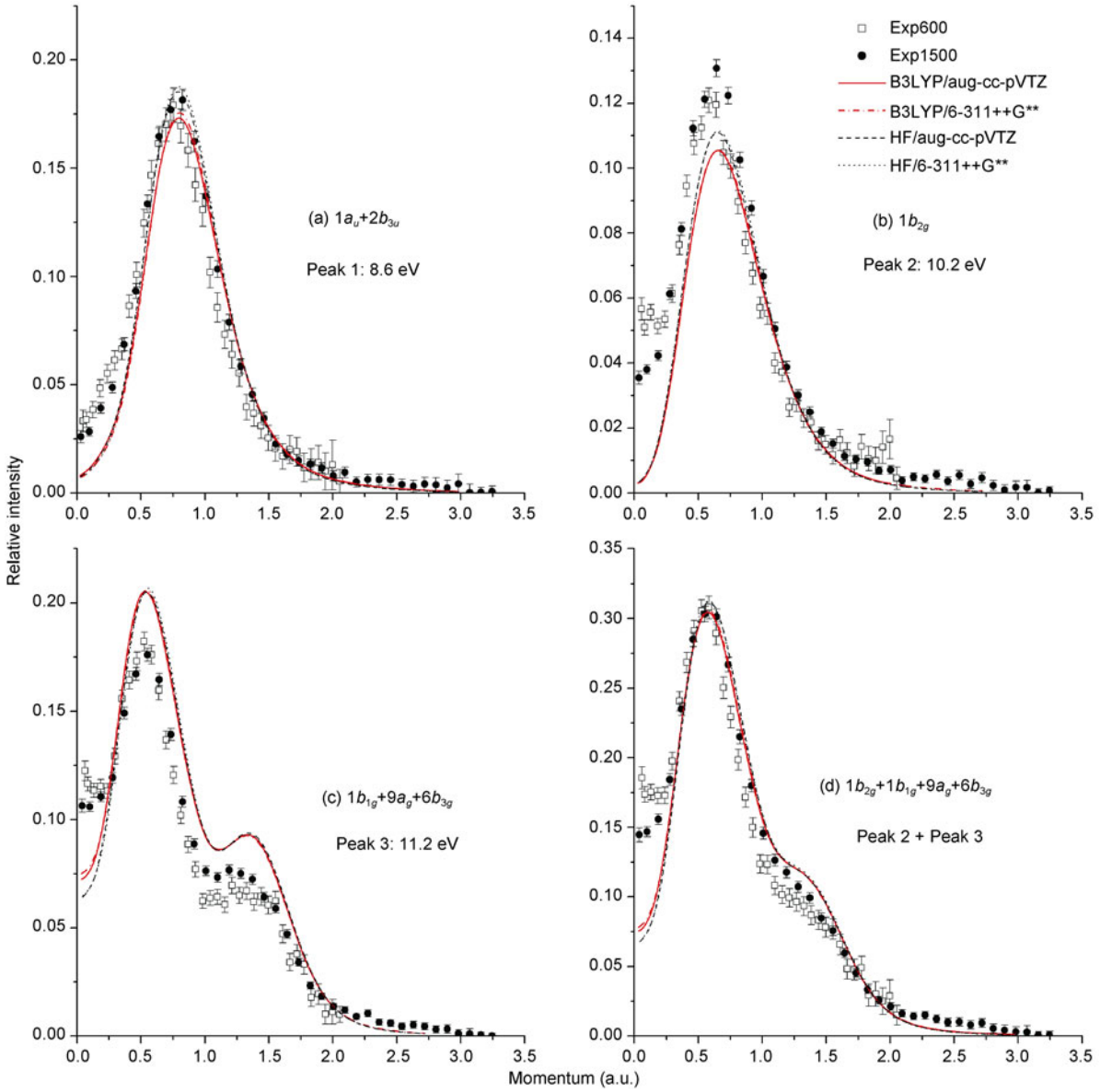

Figure 2 (Color online) The experimental and calculated momentum distributions for peak 1, peak 2 and peak 3 of naphthalene at impact energies of 600 eV and 1500 eV. The theoretical momentum profiles were calculated by using HF and DFT-B3LYP with the Aug-cc-pVTZ and 6-311++G** basis sets, respectively.

at 11.2 eV and related to three molecular orbitals: $1b_{1g}$, $9a_g$, and $6b_{3g}$. In general, the agreement between experiments and theories is reasonable except the larger discrepancy at the low momentum region. Since Peaks 2 and 3 overlapped in a considerable degree on the binding energy spectra, the summation of peak 2 and peak 3 was also compared with theoretical calculations in Figure 2(d).

Although the theoretical and experimental data in this figure are consistent in the higher momentum region, the "turn up" phenomena in the low momentum area ($p < 0.25$ a.u.) still exist. On the other hand, the discrepancy in the lower momentum region for both peaks was reduced as the impact energy increased from 600 eV to 1500 eV. Considering the similar phenomenon which has been observed in the atomic d orbitals and some molecular orbitals [24–30], such as ethylene [29] and oxygen [30] before, the most likely explanation is the distorted wave effects. The distorted wave effects will be reduced as the impact energies of electrons increase because the incoming electron and outgoing electrons will be less influenced by the residual ion's potential. Moreover, as Figure 3 shows, $1a_u$, $2b_{3u}$, $1b_{2g}$ and $1b_{1g}$ have characteristics of π^* orbitals. Thus, the observed "turn up" effects in the low p region of peak 1, peak 2 and peak 3 are attributed to the distorted wave effects. Furthermore, the experimental distribution of impact energies 1500 eV matches more with the four theoretical calculations than with that of 600 eV in both Figures 2 and 3, which is also a support for the distorted wave effects explanation. At the

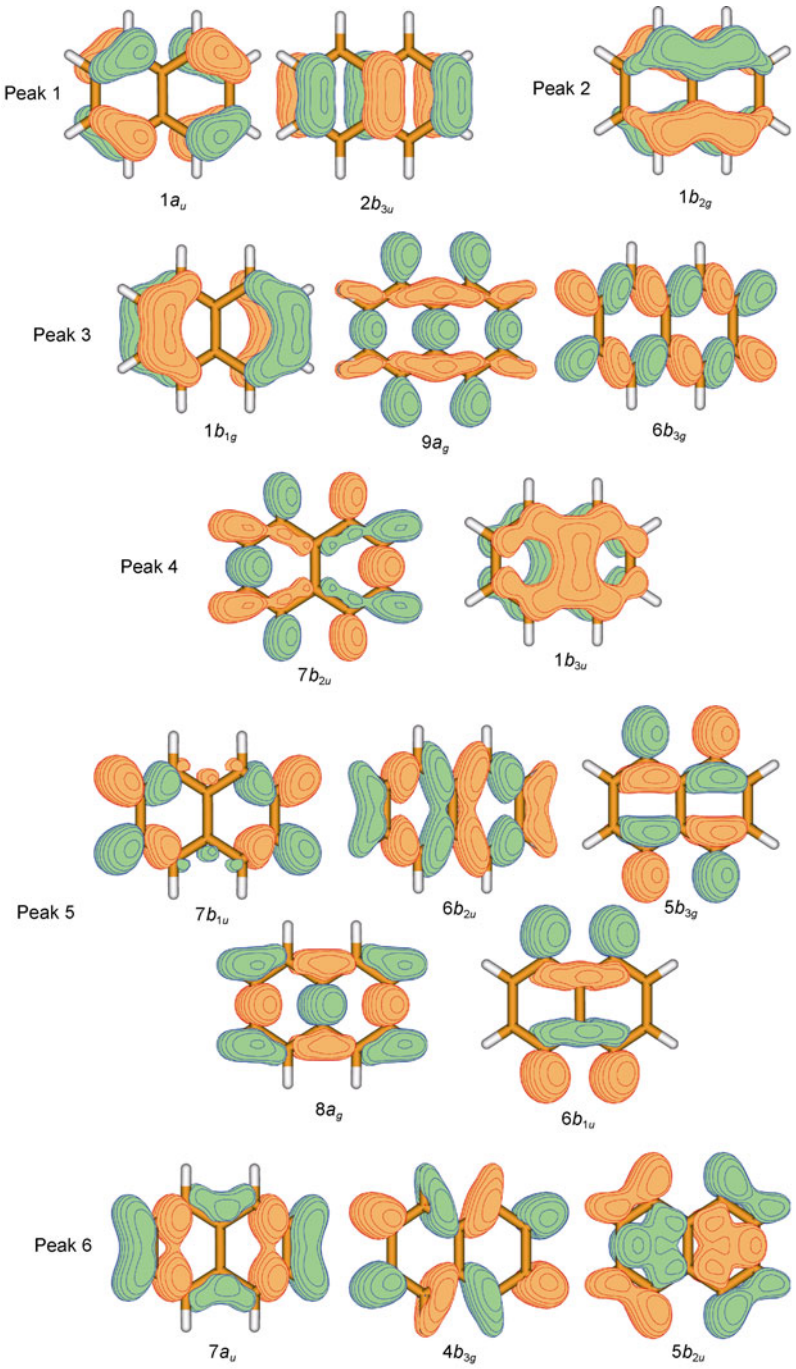

Figure 3 (Color online) The density contour plots of outer valence orbitals of naphelene. The displayed molecular orbitals were drawn using Molden 4.3 with a density contour value of 0.12 [31].

current stage, the theoretical calculation with the distorted wave approximation is still a challenge due to the multi-center and the molecular size of naphthalene [32–34].

Peak 4, peak 5 and peak 6 were assigned to $7b_{2u}$+$1b_{3u}$, $7b_{1u}$+$5b_{3g}$+$7b_{1u}$+$6b_{2u}$+$8a_g$, and $4b_{3g}$+$7a_g$+ $5b_{2u}$, respectively. Their experimental momentum distributions were compared with four theoretical calculations using HF and DFT-B3LYP with the Aug-cc-pVTZ and 6-311++G** basis sets in Figure 4. Generally speaking, all theoretical calculations can produce the overall shapes of experimental distributions, but there are some evident discrepancies in the low momentum region. One possible explanation is still the distorted wave effects because there is better agreement at higher impact energy 1500 eV.

Figure 4(d) shows the momentum distributions of peak 7 which is related to $6a_g$, $5b_{1u}$ and $4b_{2u}$ orbitals in the inner valence. The experimental pole strengths of these three orbitals are 0.75, noticeably less than 1.0, indicating the breakdown of orbital pictures in the inner valence region [22].

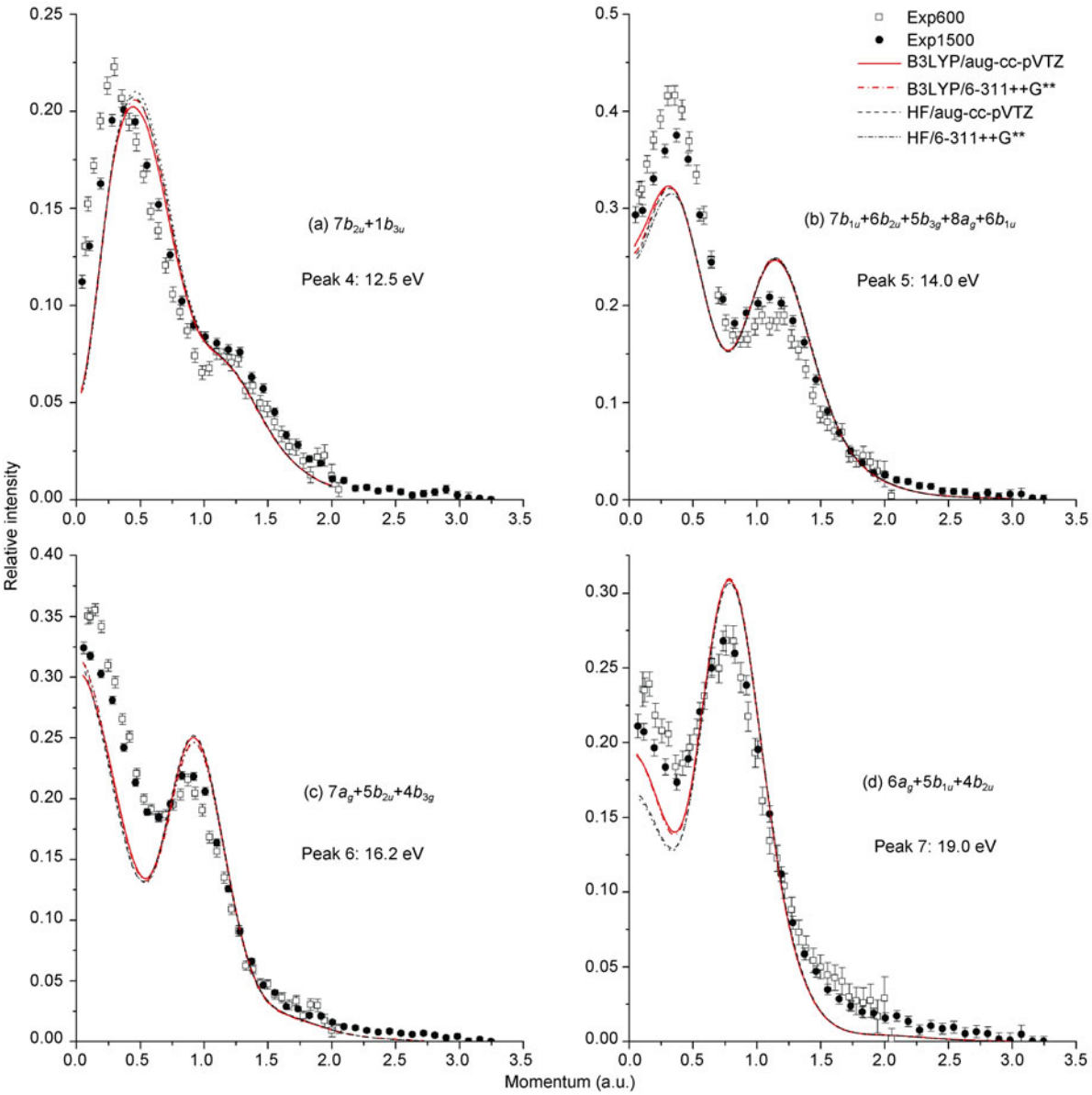

Figure 4 (Color online) The experimental and calculated momentum distributions for peak 4(a), peak 5(b), peak 6(c) and peak 7(d) of naphthalene at impact energies of 600 eV and 1500 eV. The theoretical momentum profiles were calculated by using HF and DFT-B3LYP with the Aug-cc-pVTZ and 6-311++G** basis sets, respectively.

For a better description of the big hump in the inner valence area, four Gaussian functions are used to fit peak 8, as shown in Figure 1(b). The four Gaussian functions labeled λ, μ, ν and ξ were assigned to $3b_{3g}$+$5a_g$, $4b_{1u}$, $3b_{2u}$ and $5a_g$, respectively. Their experimental momentum distributions were compared with four theoretical calculations in Figure 5. It can be inferred that the momentum distributions of peak λ take on *sp*-type characteristics, and peak μ and peak ν are of *p*-type, and peak ξ is of *s*-type. The experimental pole strengths of these orbitals are 0.44, 0.4, 0.44 and 0.14, noticeably less than 1.0. This also indicates the breakdown of orbital pictures in the inner valence region [22].

5 Conclusions

In summary, we report the full valence shell binding spectra and orbital momentum profiles of the naphthalene. The experimental momentum distributions were compared with the theoretical momentum calculations using HF and DFT methods with both Aug-cc-pVTZ and 6-311++G** basis sets. In general, the experimental results were well described by the HF and DFT calculations under PWIA except the low momentum region. Since the discrepancy was reduced as the impact energy increased, we ascribed it to the distorted wave effects.

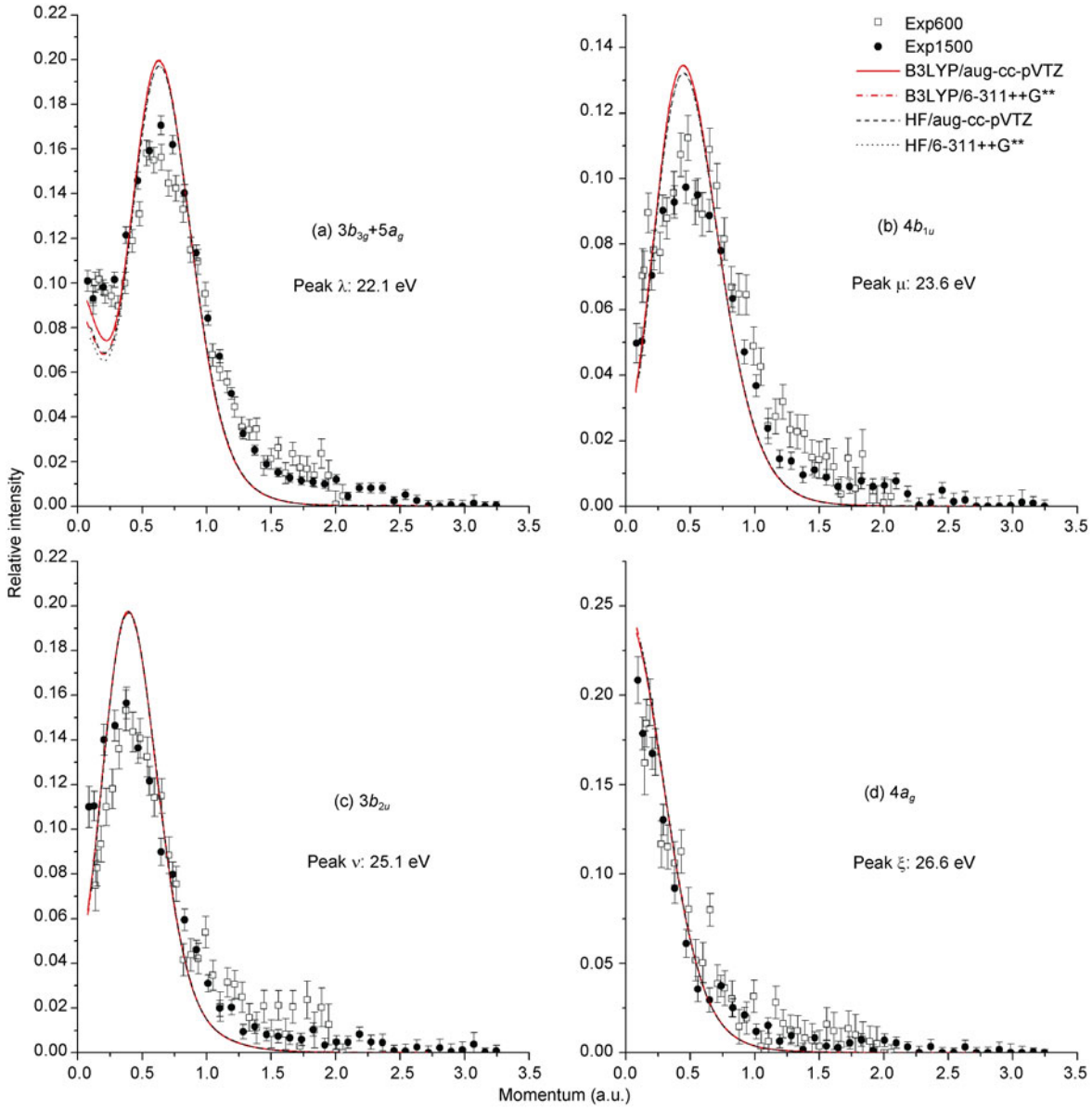

Figure 5 (Color online) The experimental and calculated momentum distributions for the inner valence orbitals of peak 8 at impact energies of 600 eV and 1500 eV. The theoretical momentum profiles were calculated by using HF and DFT-B3LYP with the Aug-cc-pVTZ and 6-311++G** basis sets, respectively.

This work was supported by the National Natural Science Foundation of China (Grants Nos. 11074144, 10874097 and 10704046) and Specialized Research Fund for the Doctoral Program of Higher Education (Grant No. 20070003146).

1 Mccarthy I E, Weigold E. Electron momentum spectroscopy of atoms and molecules. Rep Prog Phys, 1991, 54: 789–879
2 Coplan M A, Moore J H. Doering J P. (e, 2e) spectroscopy. Rev Mod Phys, 1994, 66: 985–1014
3 Weigold E, McCarthy I E. Electron Momentum Spectroscopy. New York: Kluwer Academic Plenum Publishers, 1999
4 Klevens H B, Platt J R. Spectral resemblances of cata-condensed hydrocarbons. J Chem Phys, 1949, 17: 470–481
5 Vanbrunt R J, Wacks M E. Electron-impact studies of aromatic hydrocarbons.3. Azulene + Naphthalene. J Chem Phys, 1964, 41: 3195–3199
6 Munakata T, Ohno K, Harada Y, et al. Assignment of photo-electron bands for naphthalene and anthracene by penning ionization electron-spectroscopy. Chem Phys Lett, 1981, 83: 243–245
7 Yamauchi M, Yamakita Y, Yamakado H, et al. Collision energy resolved Penning ionization electron spectra of polycyclic aromatic hydrocarbons. J Electron Spectrosc Relat Phenom, 1998, 88: 155–161
8 Jochims H W, Rasekh H, Ruhl E, et al. The photofragmentation of naphthalene and azulene monocations in the energy-range 7-22 Ev. Chem Phys, 1992, 168: 159–184
9 Rink J E, Boesl U. Mass-selected resonance-enhanced multiphoton ionisation spectra of laser-desorbed molecules for environmental analysis: 16 representative polycyclic aromatic compounds. Eur J Mass Spectrom, 2003, 9: 23–32
10 Dunning T H. Gaussian-basis sets for use in correlated molecular calculations. 1. The atoms boron through neon and hydrogen. J Chem

Phys, 1989, 90: 1007–1023
11 Krishnan R, Binkley J S, Seeger R, et al. Self-consistent molecular-orbital methods.20. Basis set for correlated wave-functions. J Chem Phys, 1980, 72: 650–654
12 Brion C E. Looking at orbitals in the laboratory—the experimental investigation of molecular wave-functions and binding-energies by electron momentum spectroscopy. Int J Quantum Chem, 1986, 29: 1397–1428
13 Duffy P, Chong D P, Casida M E, et al. Assessment of kohn-sham density-functional orbitals as approximate dyson orbitals for the calculation of electron-momentum-spectroscopy scattering cross-sections. Phys Rev A, 1994, 50: 4707–4728
14 Ren X G, Ning C G, Deng J K, et al. (e, 2e) electron momentum spectrometer with high sensitivity and high resolution. Rev Sci Instrum, 2005, 76: 063103
15 Ning C G, Zhang S F, Deng J K, et al. Improvements on the third generation of electron momentum spectrometer. Chin Phys B, 2008, 17: 1729–1737
16 Vonniessen W, Schirmer J, Cederbaum L S. Computational methods for the one-particle Green-function. Comput Phys Rep, 1984, 1: 57–125
17 Ortiz J V. Electron-binding energies of anionic alkali-metal atoms from partial 4th-order electron propagator theory calculations. J Chem Phys, 1988, 89: 6348–6352
18 Cederbaum L S. One-body greens function for atoms and molecules—theory and application. J Phys B-At Mol Opt Phys, 1975, 8: 290–303
19 Ortiz J V. Partial 4th order electron propagator theory. Int J Quantum Chem, 1988, 431–436
20 Zakrzewski V G, Ortiz J V. Semidirect algorithms for 3rd-order electron propagator calculations. Int J Quantum Chem, 1995, 53: 583–590
21 Chong D P, Gritsenko O V, Baerends E J. Interpretation of the Kohn-Sham orbital energies as approximate vertical ionization potentials. J Chem Phys, 2002, 116: 1760–1772
22 Cederbaum L S, Domcke W. Localized and delocalized core holes and their interrelation. J Chem Phys, 1977, 66: 5084–5086
23 Duffy P, Casida M E, Brion C E, et al. Assessment of gaussian-weighted angular resolution functions in the comparison of quantum-mechanically calculated electron momentum distributions with experiment. Chem Phys, 1992, 159: 347–363
24 Brion C E, Zheng Y, Rolke J, et al. Distorted-wave effects at low momentum in binary (e, 2e) cross sections for d-orbital ionization. J Phys B-At Mol Opt Phys, 1998, 31: L223–L230
25 Zhang X H, Chen X J, Xu C K, et al. An electron momentum spectroscopy study of the outer valence orbitals of chlorodifluoromethane. Chem Phys, 2004, 299: 17–24
26 Brunger M J, Braidwood S W, Mccarthy I E, et al. An electron momentum spectroscopy investigation of the 4d core states of xenon. J Phys B-At Mol Opt Phys, 1994, 27: L597–L601
27 Takahashi M, Saito T, Hiraka J, et al. The impact energy dependence of momentum profiles of glyoxal and biacetyl and comparison with theory at their high-energy limits. J Phys B-At Mol Opt Phys, 2003, 36: 2539–2551
28 Ren X G, Ning C G, Deng J K, et al. (e,2e) study on distorted-wave and relativistic effects in the inner-shell ionization processes of xenon 4d(5/2) and 4d(3/2). Phys Rev A, 2006, 73: 042714
29 Ren X G, Ning C G, Deng J K, et al. Direct observation of distorted wave effects in ethylene using the (e,2e) reaction. Phys Rev Lett, 2005, 94: 163201
30 Ning C G, Ren X G, Deng J K, et al. Turn-up effects at low momentum for the highest occupied molecular orbital of oxygen at various impact energies by electron momentum spectroscopy. Phys Rev A, 2006, 73: 022704
31 Schaftenaar G, Noordik J H. Molden: A pre- and post-processing program for molecular and electronic structures. J Comput Aided Mol Des, 2000, 14: 123–134
32 Gao J F, Madison D H, Peacher J L. Interference effects for low-energy electron-impact ionization of nitrogen molecules. Phys Rev A, 2005, 72: 032721
33 Colyer C J, Stevenson M A, Al-Hagan O, et al. Dynamical (e, 2e) studies of formic acid. J Phys B-At Mol Opt Phys, 2009, 42: 235207
34 Hargreaves L R, Colyer C, Stevenson M A, et al. (e, 2e) study of two-center interference effects in the ionization of N-2. Phys Rev A, 2009, 80: 062704